Accelerated soil nitrogen cycling in response to a whole ecosystem acid rain mitigation experiment

Richard E. Marinos[a,b]*, Peter M. Groffman[c,d], Charles T. Driscoll[e] and Emily S. Bernhardt[a,f]

[a]Nicholas School of the Environment, Duke University, Durham, NC, USA

[b]Department of Geology, The University at Buffalo, Buffalo, NY, USA, rmarinos@buffalo.edu

[c]Cary Institute of Ecosystem Studies, Millbrook, NY, USA

[d]City University of New York Advanced Science Research Center at the Graduate Center, New York, NY, USA, peter.groffman@asrc.cuny.edu

[e]Department of Civil and Environmental Engineering, Syracuse University, Syracuse, NY, USA, ctdrisco@syr.edu

[f]Department of Biology, Duke University, Durham, NC, USA, emily.bernhardt@duke.edu

*Corresponding author: Richard Marinos, rmarinos@buffalo.edu, 126 Cooke Hall, Buffalo, NY 14260

Abstract

Acid deposition has declined substantially over the last thirty years in the developed world. In forested watersheds previously impacted by acid deposition, evidence suggests that soils are slowly beginning to recover their alkalinity and base cation fertility. Research in these recovering ecosystems suggests that these changes in soil chemistry may result in decreased ecosystem retention and greater hydrologic export of nitrogen (N), although the drivers behind this enhanced export remain poorly understood. A whole-watershed acid rain mitigation experiment at Hubbard Brook Experimental Forest (New Hampshire, USA) offers a unique opportunity to examine how forest N cycling might change as soil recovery progresses further over the coming decades. In this experiment, researchers added 1168 kg ha^{-1} of wollastonite ($CaSiO_3$) to an 11.8 ha watershed in 1999, leading to sustained increases in soil pH and increasing Ca fertility. By 2008, the experimental watershed began to export significant quantities of nitrogen, becoming a net nitrogen source for the first time since measurements began in 1963. We sought to understand whether shifts in soil N cycling could explain this watershed phenomenon. Across repeated soil sampling campaigns in 2015 and 2016, we found that soil inorganic nitrogen pools in the treated watershed were between 1.8 and 2.6 times higher ($p < 0.001$) than in a nearby reference watershed. Gross N mineralization rates and immobilization rates were ~40% higher in the litter layer (Oie horizon) of the treated watershed as well ($p < 0.001$). We conclude that an accelerated N cycle in this litter layer, with faster turnover between organic and inorganic N pools, likely resulted in faster replenishment of inorganic N pools that were susceptible to hydrologic loss, resulting in higher N export. Nitrogen

cycling rates were uncorrelated with soil acid-base properties, suggesting that direct geochemical controls are not the primary driver of the altered N cycle.

Key Words

nitrogen cycle, acid rain, nitrogen mineralization, temperate hardwood forest, calcium

1. ***Introduction***

Soil acidity modifies the bioavailability of organic matter and determines both the structure and activity of soil microbial communities, thus playing a central role in mediating coupled soil carbon (C) and nitrogen (N) dynamics (Schmidt et al. 2011, Coughlan et al. 2000, Rousk et al. 2009, Illmer et al. 2003). Despite the importance of acidity as a master driver of soil biogeochemical cycling, the impacts of rapid changes (i.e. over decades to centuries) in soil acidity are seldom considered in long-term projections of ecosystem dynamics. This is a critical knowledge gap, because while soil acidity is generally stable over millennial timescales in the absence of human activities (Slessarev et al. 2016), anthropogenic acid deposition (hereafter referred to as 'acid rain') has caused severe soil acidification over the past century (Likens et al. 1996). Over the last few decades, clean air regulations in the developed world have resulted in substantial reductions in soil acidity in previously-impacted areas (Kirk et al. 2010, Lawrence et al. 2012, Lawrence et al. 2015). These rapid decreases in soil acidity have been linked to declines in soil organic matter (Oulehle et al. 2011, Lawrence et al. 2015) and increased hydrologic export of dissolved organic carbon (Monteith et al. 2007, Erlandsson et al. 2011). Importantly, decreases in soil acidity have also been linked to increases in watershed inorganic N export, despite the fact that decreases in soil acidity are substantially driven by decreases in nitric acid deposition (Lawrence et al. 2020). Although there are many mechanisms by which changing soil acidity may alter soil C and N cycling, process-based biogeochemical models (e.g. DayCent, CLM-CN, Biome-BGC) generally do not explicitly include any links between soil acidity and C and N process rates (Thornton 2005, Parton et al. 1998; Oleson et al. 2013). Understanding long-term trajectories of ecosystem recovery from acid rain, and their implications for global C and N

stocks, will require a more thorough understanding of how rapid anthropogenic changes in soil acidity affect ecosystem C and N storage, cycling, and loss.

There are a variety of mechanisms through which historical soil acidification, and current trends of deacidification, are likely to impact ecosystem biogeochemistry. Several dominant tree species have proven very sensitive to soil acidity, and their declines with soil acidification may be reversed as ecosystems recover. In eastern North America, the depletion of soil calcium (Ca) throughout acid rain impacted regions has been linked to declines in sugar maple (*Acer saccharum*) and red spruce (*Picea rubra*) (Joslin et al. 1992, Sullivan et al. 2013). It has been proposed that the decline in sugar maple may lead to substantial changes in soil biogeochemical processes, since sugar maple litter is of higher quality than the majority of other tree species throughout their range (Lovett et al. 2002, Hobbie et al. 2007). Furthermore, increased litter calcium content has been shown to be directly correlated with higher rates of litter decomposition (Grossman et al. 2020), although in other cases calcium addition been associated with higher microbial carbon-use efficiency and reduced litter turnover (Shabtai et al. 2023).

In addition to changes in the quality of litter inputs to the soil, ecosystem acidification has direct effects on belowground biogeochemical cycling. Acidification may result in greater stabilization of soil organic matter (SOM), reducing C and N mineralization, and deacidification may conversely destabilize this SOM (Bailey et al. 2019). This increased stabilization in acid soils results from reduced organic matter solubility, enhanced association between protonated organic molecules and mineral surfaces, and increased complexation with aluminum (Al) (Clarholm and Skyllberg 2013, SanClements et al. 2018, Hall and Thompson 2022). Conversely, acidification may reduce stabilization of SOM by calcium, which has recently been shown to be a mechanism of stabilization even in naturally acidic soils (Rowley et al. 2018, Rowley et al.

2023). Whether SOM is stabilized or destabilized as a result of changes to soil acidity is likely to depend on how these mechanisms of SOM stabilization are influenced by the initial soil pH and the magnitude of pH change.

In addition to stabilizing SOM, high soil acidity has also been shown to inhibit soil microbial activity (Illmer et al. 2003, Jones et al. 2019, Niemi and Vepsalienen 2005) and to alter the abundance and composition of microbial guilds responsible for key pathways in soil N cycling (Simek and Cooper 2002, Liu et al. 2010, Stempfhuber et al. 2015). A recent global meta-analysis demonstrates that decreased soil pH limits gross nitrogen mineralization, both directly and indirectly via impacting microbial biomass (Elrys et al. 2021). Nitrification is also known to be inhibited by high soil acidity (Mueller et al. 2012, Li et al. 2018, but see Venterera et al. 2004), and nitrification is a key pathway by which N is mobilized and lost from ecosystems (Likens et al. 1969). Finally, soil acidification can decrease soil faunal activity and the associated decomposition of SOM (Reich et al. 2005, Geissen and Brummer 1999). Though there are multiple pathways through which soil acidity can affect above- and belowground C and N cycling (Rousk et al. 2009), most of them are consistent with acidification resulting in a reduced potential C and N turnover in soil. Thus, as ecosystems recover from acid rain, C and N cycling may accelerate, though the extent of this acceleration remains an open question.

In 1999, a watershed acid mitigation experiment, performed at Hubbard Brook Experimental Forest (HBEF), induced profound changes in watershed C and N cycling, changes that might foreshadow processes that will occur as forest ecosystems gradually recover from acid rain over the coming decades (Johnson et al. 2014, Rosi-Marshall et al. 2016). HBEF experienced substantial acid deposition since the Industrial Revolution, but this deposition has largely abated due to the success of air pollution regulation, such that, by the time of this study,

annual sulfuric acid deposition was 89% lower and nitric acid deposition was 68% lower than their respective peaks in the mid-1970s (Likens 2013, Hubbard Brook Watershed Ecosystem Record 2021). Nonetheless, HBEF experiences important continuing legacies of over a hundred years of historical acid deposition, including depressed soil pH and cationic nutrient fertility. In this 1999 experiment, calcium silicate ($CaSiO_3$) was applied via helicopter to an 11.8 ha watershed to elevate soil Ca by 1168 kg ha^{-1} and increase soil pH (full details of the experiment in Johnson et al. 2014).

In the decade following the treatment, sugar maple biomass and litterfall increased (Battles et al. 2014), as did total leaf and leaf litter N content (Lovett et al. 2016, Juice et al. 2006). These increases in aboveground biomass C and N were accompanied by much larger, contemporaneous decline in shallow soil C and N stocks of 35% and 31%, respectively. (Johnson et al. 2014). While these substantial shifts in aboveground and belowground C and N pools occurred within the first several years of treatment, soil solution N fluxes and whole watershed N exports did not increase substantially until much later. From 1999 to 2007, watershed N export in the Ca-enriched watershed roughly followed the declining trend that was likewise observed in the reference watershed, and which tracked declines in atmospheric N deposition (Likens 2013). Watershed N export began to increase abruptly beginning in 2008, such that, by 2013, watershed N export was thirty times higher than the reference watershed (Rosi-Marshall et al. 2016). Such a dramatic increase in watershed N exports must be the result of altered soil N cycling rates associated with the loss of SOM pools, yet early in the experiment (2000-2002), Groffman et al. (2006) measured no significant treatment effects on gross or net N cycling in the Ca-enriched watershed. Routine summer measurements of net N mineralization and nitrification, which continued into the period of high watershed N export, have similarly

shown no response to watershed treatment (Groffman 2021). Thus, the sources of this increased N export remain unresolved.

Here, we addressed three hypotheses that may reconcile the observations of significant watershed N loss in the absence of any measurable changes in net soil N cycling rates (Rosi-Marshall et al. 2016, Groffman 2021) and may offer an explanation for the long lag between the $CaSiO_3$ treatment and the watershed N export response. First, we hypothesized that although the treatment enhanced rates of microbial N mineralization, this effect was counterbalanced by enhanced biotic demand for N. If both enhanced mineralization and immobilization result from this acid mitigation experiment, this would result in an accelerated N cycle without any change in net process rates. A faster N cycle could lead to higher watershed N exports if hydrologic flushing regularly leaches N from this high-turnover pool. There are two hypotheses that may explain the decade long lag between watershed treatment and enhanced nitrogen export. The first is that gradual increases in litter quality (Juice et al. 2006, Lovett et al. 2016) are resulting in faster N turnover in organic soil horizons. The second is that documented losses of soil organic matter throughout the soil profile are the source of this excess N, and that the delayed delivery of surface-applied $CaSiO_3$ to deeper horizons explains the lag. We examined each of these hypotheses by measuring both gross and net nitrogen mineralization and nitrification rates throughout the soil profile during two sampling campaigns. These sampling campaigns occurred during early spring and summer, time periods that capture the extremes of biotic demand for inorganic N, relative to supply (Pardo et al. 2005, Judd et al. 2007).

2. Methods

2.1 Site description

Hubbard Brook Experimental Forest (White Mountains NF, New Hampshire, USA) is primarily a mixed hardwood forest composed of American beech (*Fagus grandifolia*), sugar maple (*Acer saccharum*), and yellow birch (*Betula allegheniensis*), with some conifers at higher elevations. Soils are well-drained podzols formed on unsorted glacial till parent material, with a mean depth to bedrock of ~2 m (Johnson et al. 2014). The topography is steep, with the study area having a mean slope of 17º and an elevation between 400 and 800 m (Groffman et al. 2006). The landscape microtopography at HBEF is characterized by pit-and-mound features caused by tree wind throws. These depressional pits have been shown elsewhere to play an important role in seedling recruitment, greenhouse gas fluxes, pedogenesis, and hydrologic routing (Schaetzl et al. 1988, Veneman et al. 1984, Phillips et al. 2017, Kooch et al. 2015, Valtera and Schaetzl 2017).

The study was conducted in two small watersheds within HBEF in a paired watershed experimental design. In October 1999, one watershed (Ca-enriched watershed) was treated with powdered, pelletized wollastonite ($CaSiO_3$) with the goal of replacing soil Ca lost due to anthropogenic acid deposition. The other watershed, located immediately to the west of the long-term biogeochemical reference watershed at HBEF, was maintained as a control (reference watershed). In the Ca-enriched watershed, base saturation of the soil increased from 10% pre-treatment to 19% post-treatment in mineral soil horizons, and the treatment had a complex but overall positive effect on soil pH, which is explored more fully by Johnson et al. (2014).

2.2 Soil collection

Soil collection sites were established at six sites within the hardwood vegetation zones of each watershed. In the Ca-enriched watershed, sites were selected immediately downslope of lysimeters which were installed in random locations throughout the watershed as part of a long-term monitoring program (Cho et al. 2010). In the reference watershed, sites were selected randomly using ArcGIS. Because of the potential importance of pit and mound microtopography in driving biogeochemical processes, we explicitly sampled across this gradient, establishing at each site two plots that spanned the range of pit-and-mound microtopography. One plot was established in a depressional area believed to be a relict pit from an old tree throw, and the other was established on an adjacent convex area thought to be a relict mound. Fresh pit and mounds (those with still-visible root masses) were not sampled. Thus, each watershed contained a total of twelve sampling plots, six in depressional landforms and six in convex landforms.

Soils were sampled on two occasions within each plot, during the peak growing season in early August 2015 (summer) and after snowmelt but before leaf-out in late March 2016 (spring). The former sampling time corresponds to the time period of lowest N flux from watersheds at HBEF, and the latter corresponds to the period of high N flux, a seasonal pattern that has been attributed to the relative demand of vegetation for N (Likens 2013). On both occasions, sampling occurred 2 - 3 days after a significant rainstorm, and soils were at or near field capacity. Soils were collected, bulked by horizon (Oie, Oa, and 0-10 cm mineral soil), and homogenized using the methods that Groffman (2021) employed for long-term soil monitoring at HBEF. Soils used for microbial process rate measurements were stored at 4ºC until analysis, which occurred within ten days of sample collection. A subsample of each soil was air-dried and stored for later analysis of soil pH and exchangeable cations.

2.3 Laboratory analysis

The water content of both field-moist and air-dry soils was determined by gravimetric moisture loss after drying at 60 ºC for 48 h in a drying oven. Soil organic matter (SOM) content was determined by mass loss on ignition at 550 ºC for 4h in a muffle furnace. Soil pH was measured potentiometrically in a 2:1 water : soil slurry using a Mettler-Toledo DL-18 probe. Exchangeable base cations were extracted from 5g of air-dry soil using 50 ml of 1M ammonium acetate buffered to pH 7. These slurries were rotated at 60 rpm on an end-over shaker for 24h, then vacuum filtered through a Gelman A/E glass fiber filter (1.0 μm nominal pore size). All samples were analyzed for exchangeable Ca on a Perkin Elmer 3100 Flame AA spectrometer, and the spring 2016 samples were further analyzed for K, Mg, and Na. For spring 2016 samples, exchangeable acidity and aluminum (Al) were extracted from 10g of field moist soil (5g for Oie horizon soil) using 50 ml of 2 M potassium chloride, shaken at 120 rpm for 1 h on a shaker table, and gravity filtered through a pre-rinsed Whatman 42 filter (2.5 μm nominal pore size). Exchangeable acidity and exchangeable Al were determined titrimetrically following the method in Abreu et al. (2003), using a Mettler-Toledo DL-18 autotitrator. Cation exchange capacity and base saturation were calculated by summation (Robertson et al. 1999).

Soil ammonium (NH_4^+) and nitrate (NO_3^-) pool sizes were determined by extraction of 10 g of field moist soil (5 g for Oie horizon soil) using 50 ml of 2 M potassium chloride, shaken at 120 rpm for 1 h on a shaker table and gravity filtered through a pre-rinsed Whatman 42 filter. These extracts were analyzed colorometrically on a Lachat QuikChem flow injection analyzer. To measure potential C mineralization, net N mineralization, and net nitrification, we performed short-term laboratory soil incubations. Field moist soil (10 g for Oa and mineral horizon soils, 5 g for Oie horizon soil) was incubated in the dark for 10 d at 20 ºC in a 976 ml glass jar fitted with

a butyl rubber septum. After the incubation, headspace gas was sampled with a 1 ml gas syringe. This gas sample was immediately analyzed for CO_2 concentration using a Li-Cor LI-6200 IRGA in a flow injection configuration. C mineralization potential on a basis of per gram of dry soil per day was calculated from accumulation of headspace CO_2 over the course of the incubation. After headspace gas analysis, the samples were analyzed for NH_4^+ and NO_3^- following the same procedure outlined above. Net N mineralization was calculated as the net increase of NH_4^+-N and NO_3^--N over the course of the incubation, and net nitrification as the net increase of NO_3^--N only, each expressed on a per gram of dry soil per day basis. Microbial biomass was measured by the chloroform fumigation-incubation method (Jenkinson and Powlson 1976), with CO_2 production measured in the same manner as in the C mineralization assays.

For samples from the spring 2016 sampling date, we used a laboratory isotopic pool dilution approach to measure potential gross N mineralization, nitrification, and N immobilization, slightly modifying the protocol used by Groffman et al. (2006). Four replicate 10 g subsamples of each soil (5 g for Oie horizon soil) were weighed into specimen cups and pre-incubated for 12h. Two of these subsamples were then amended with 45 μg of 99 atom % ^{15}N as $^{15}NH_4Cl$ for measurement of gross N mineralization, and two subsamples were amended with 45 μg ^{15}N as $K^{15}NO_3$ for measurement of gross nitrification. The amendments were dissolved in 1 ml of water that was sprayed slowly onto the soil through a 28 ga. needle while constantly tumbling the sample to homogenize the application. In order to determine initial pool sizes and isotopic compositions of the soil inorganic N pools, we extracted inorganic N from one of the $^{15}NH_4^+$-amended samples and one of the $^{15}NO_3^-$-amended samples within fifteen to thirty minutes after the labeled N amendment, using the KCl extraction procedure described above. The remaining samples were incubated for 3 d at 20 ºC in the dark and then extracted following

the same protocol. NH_4^+ and NO_3^- concentrations were determined by colorometric analysis on a Lachat QuikChem flow injection analyzer. Samples were prepared for isotopic analysis using a diffusion/acid trap method similar to Sorensen and Jensen (1991). The isotopic composition of the samples was measured by EA-IRMS at the Stable Isotope Facility at UC-Davis. Gross process rates were calculated from initial and final pool sizes and isotopic compositions using the equations in Hart et al. (1994).

2.4 Statistical analysis

All statistical analyses were performed in R v. 4.2.1 (R Core Team, 2022). To test for differences between watersheds for parameters of interest, we performed blocked one-way ANOVA analyses, with microtopographic position included as a blocking factor. The blocking factor was significant for only 3 out of 69 statistical comparisons performed, below the expected 5% false discovery rate under the null hypothesis of no difference between blocking factor levels, but the blocking factor was nonetheless retained in all models. We analyzed each season and each soil horizon separately. We also fit linear models to test for correlations between soil geochemical properties (pH, base saturation, exchangeable Ca, exchangeable Al) and soil microbial processes. To examine whole-profile soil inorganic N pools, we scaled soil concentration measurements by the mean soil horizon masses reported for each watershed (Johnson and Hamburg 2016, Johnson et al. 2014). We report statistically significant results at $\alpha = 0.10$.

To contextualize our findings regarding soil N process rates, we prepared a N budget "snapshot" for the leaf litter horizon (Oie) during the spring sampling campaign. To estimate field N process rates at springtime soil temperatures, we scaled our potential rate measurements obtained at 20 ºC to expected rates at 5 ºC, based on a Q10 of 2.5, a value reported for organic

horizon podzols by Katterer et al. (1998). The organic N pool size in the Oie horizon for the Ca-enriched watershed was taken from Johnson et al. (2014), and the pool size in the reference watershed was computed from soil horizon mass and % C data from Johnson and Hamburg (2016), assuming the same C:N ratio as in the Ca-enriched watershed. Leaf litter inputs were calculated using leaf litter mass data from Fahey (2016) and litter chemistry data from Lovett et al. (2016). Root litter inputs were estimated from fine root mass data from Fahey et al. (2016), root turnover rates estimated from Tierney and Fahey (2002) and root N concentration data from Fahey et al. (1994). Microbial biomass N was computed with data from Groffman (2016) and Johnson et al. (2014). N deposition estimates were taken from Rosi-Marshall et al. (2016).

We further contextualized our work by examining how soil solution fluxes of inorganic nitrogen have changed since the early period of the Ca enrichment experiment. To determine if altered rates of microbial N processing were the likely driver of enhanced watershed N export, we calculated vertical soil solution fluxes of inorganic nitrogen through the organic and mineral soil horizons using soil solution data from zero tension lysimeter nests sampled monthly in the Ca-enriched (n=13) and reference (n=3) watersheds. These fluxes were calculated by multiplying soil solution inorganic N concentrations by the estimated monthly hydrologic flux, calculated using the PnET-BGC model (Gbondo-Tugbawa et al., 2001).

3. Results

Seventeen years after the initial treatment, soil acid-base status remained strongly impacted by $CaSiO_3$ treatment in the organic soil horizons, with a more muted response in the mineral soil (Figure 1). Topographic position and season had no significant effect on these soil properties. In the Ca-enriched watershed, soil pH was 0.26 units higher in the Oie horizon ($p < 0.001$) and 0.15 units higher in the Oa horizon ($p = 0.006$), compared to the reference watershed.

In the mineral soil, we did not detect a significant difference in soil pH. Exchangeable Al was 86% lower in the Oie horizon *($p = 0.033$*) and 38% lower in the Oa horizon ($p = 0.030$), but was not significantly different in the mineral soil. Exchangeable Ca was 2.2-fold higher in the Oie Horizon ($p < 0.001$), 5.6-fold higher in the Oa horizon ($p<0.001$), and 5.7-fold higher in the mineral horizon ($p < 0.001$). Base saturation was significantly higher in the Ca-enriched watershed in all horizons; in the Oie horizon, mean base saturation was 89.8% in the Ca-enriched watershed versus 77.8% in the reference watershed ($p = 0.013$), 56.3% versus 20.7% in the Oa horizon ($p < 0.001$) and 18.4% versus 9.0% in the mineral soil ($p < 0.001$).

For both sampling dates, soil inorganic N concentrations were generally higher in the Ca-enriched watershed than in the reference watershed (Figure 2). In absolute terms, the greatest differences in inorganic N concentrations between watersheds were observed in the Oie horizon, as this horizon contained, on average, 3.5 times the total inorganic N (TIN) of the Oa horizon and 12.0 times the TIN of the mineral horizon. When N concentrations in each horizon (Figure 2) were scaled to the mass of each horizon to estimate whole-profile inorganic N pools on an areal basis, NH_4^+, NO_3^-, and TIN pools were all significantly higher in the Ca-enriched watershed for both sampling dates (Figure 3). In the Ca-enriched watershed, whole-profile NH_4^+ pools were 2.5 times larger than the reference watershed during the summer ($p < 0.001$), and 2.4 times larger in the spring ($p < 0.001$); NO_3^- pools were 1.4 times larger during the summer ($p = 0.041$) and 4.1 times larger in the spring ($p < 0.001$). Summing these two pools, the TIN pool was 1.8 times larger in the Ca-enriched watershed in the summer ($p < 0.001$) and 2.6 times larger in the spring ($p < 0.001$).

Gross N cycling rates were elevated in the Ca-enriched watershed relative to the reference watershed, but there were no differences between watersheds in net N cycling rates.

Net N mineralization and nitrification were not significantly different in any soil horizon for either of the sampling dates (Figure S1). In contrast, gross N transformations were significantly higher in the Oie horizon of the Ca-enriched watershed (Figure 4). Mean potential gross N mineralization was a 98.5 (SE: ± 5.1) μg gds^{-1} in the Ca-enriched watershed and 71.8 (SE: ± 3.8) μg gds^{-1} in the reference watershed, a significant ($p < 0.001$) 37.1% difference. Mean NH_4^+ immobilization was 70.2 (SE: ± 3.3) μg gds^{-1} in the Ca-enriched watershed and 47.0 (SE: ± 3.0) μg gds^{-1} in the reference watershed, a significant ($p < 0.001$) 49.6% difference. Gross nitrification was not significantly different in the Oie horizon between watersheds, nor was NO_3^- immobilization. The difference in gross N mineralization rates, when multiplied by the greater mass of the Oie horizon in the Ca-enriched watershed, leads to an estimated 67.8% higher gross N mineralization rate and 82.8% higher NH_4^+ immobilization rate in this horizon, on an areal basis (Figure 5). There were no significant treatment effects on gross N transformations in the Oa or mineral soil horizons.

In some horizons, N cycling rates were positively correlated with soil C mineralization rates but were uncorrelated with any of the any of the soil acid-base properties we measured. Carbon mineralization and gross N mineralization were positively correlated in the Oie horizon ($r^2 = 0.305$, $p = 0.026$), weakly positively correlated in the Oa horizon ($r^2 = 0.110$, $p = 0.087$), and uncorrelated in the mineral horizon (Figure 6a). Carbon mineralization and net N mineralization were strongly positively correlated in the Oa horizon ($r^2 = 0.490$, $p < 0.001$) but uncorrelated in the Oie and mineral horizons (Figure 6b). Carbon mineralization was not significantly different between watersheds for any horizon or sampling date (Table 1). Total SOM also did not differ between watersheds (Table 1). No gross or net N cycling rates were significantly correlated with pH, exchangeable Ca, base saturation, or exchangeable Al in models

that included blocking factors for watershed, topographic position, and (where applicable) season. There were no significant differences in gross or net N mineralization or nitrification rates between microtopographic positions, either within or between watersheds, in either spring or summer (Figure S2).

Soil solution N fluxes became substantially elevated in the Ca-enriched watershed during the same time period (post-2008) that the Ca-enriched watershed began exporting much greater quantities of N (Figure 7). The greatest differences in soil solution N fluxes between the Ca-enriched and reference watersheds occurred in the organic (Oie + Oa) soil horizons, where annual N flux was a mean of 2.9 times higher (paired t-test, $p < 0.001$) in the Ca-enriched organic horizon, compared to the reference watershed organic horizon during the post-2008 period. This compares to the pre-2008 period, where N flux from the Ca-enriched organic soil horizon was only a mean 1.3 times higher ($p < 0.001$) than from the reference watershed. In the mineral horizons, annual N fluxes were 3.2 times higher in the Ca-enriched watershed in the post-2008 period and 2.0 times higher in the pre-2008 period ($p < 0.001$), although the absolute magnitudes of these fluxes are substantially smaller than those from the organic horizons.

4. Discussion

We found strong evidence of accelerated N cycling in the Ca-enriched watershed. This accelerated N cycling was only found in the leaf litter layer, although inorganic N pools were enriched throughout the soil profile. Both mineralization and immobilization were accelerated, leading to no measurable change in net mineralization rates. Net mineralization and nitrification rates were unaffected by watershed treatment, while inorganic N pools were higher in the treatment watershed in both sampling periods. Our results support the hypothesis that changes to

342 N cycling in the organic soil horizons could be sufficient to fully explain the enhanced watershed
343 N export observed in the treatment watershed (Rosi-Marshall et al. 2016).
344 The faster N turnover and larger soil inorganic N pools in the treated watershed could
345 predispose this watershed to hydrologic exports of nitrogen. Higher rates of mineralization and
346 nitrification have previously been linked to increased ecosystem losses of N (Lovett et al. 2002,
347 Phillips et al. 2013). While both gross N mineralization and gross immobilization were higher in
348 the Ca-enriched watershed in our laboratory assays, under field conditions, leaching of N is an
349 alternative fate of mineralized N, and increased N mineralization can thus drive both increased N
350 immobilization and increased leaching losses. Such a loss mechanism may be particularly
351 relevant during times when vertical water movement through the soil is slow but constant, such
352 as during spring snowmelt. While nitrification is often considered a key step in the mobilization
353 and loss of ecosystem N due to negligible retention of NO_3^- on the soil exchange complex
354 (Likens et al. 1969), ammonium can be quite mobile in acid forest soils, particularly in organic
355 horizons (Matschonat and Matzner 1995, Kothawala and Moore 2009). Enhanced nitrification
356 therefore may not be necessary to explain increased ecosystem N loss. If we extrapolate the
357 enhanced N mineralization rates in the Ca-enriched watershed (Figure 6) to an annual time step,
358 we estimate that gross annual leaf litter N mineralization would be increased by 182.5 kg ha^{-1} y^{-1}.
359 Annual N export in the Ca-enriched watershed has increased by less than 8 kg ha^{-1} y^{-1}, an
360 increase that could be explained if ~5% of this enhanced litter N mineralization is lost to
361 streamflow. We conclude that enhanced gross mineralization of N in leaf litter represents a
362 plausible mechanism to explain the observed increase in ecosystem N loss. Lysimeter data are
363 consistent with this hypothesis, documenting the greatest differences in soil solution fluxes
364 between the Ca-enriched and reference watersheds coming from the organic soil horizons

(Figure 7). This proposed mechanism is also entirely consistent with the finding that N export from the Ca-enriched watershed is considerably elevated during storms (Marinos et al. 2018).

Differences in the relationships between C mineralization and both net and gross N mineralization in each soil horizon provides additional, indirect evidence that enhanced N turnover in leaf litter (Oie horizon) may be driving inorganic N losses from this ecosystem. In leaf litter, C mineralization is positively correlated with gross N mineralization but is not correlated with net N mineralization. This discrepancy, together with the high rates of immobilization in this horizon, suggests that microbial demand for N is high in the litter layer. This is consistent with increased microbial demand for N driven by reduced N deposition, observed by others (Groffman et al. 2018). In contrast, in the underlying Oa horizon, C mineralization was strongly positively correlated with net N mineralization. This suggests that more of the N released from decomposition remains in solution, and that inorganic N is present in excess of microbial demand in this horizon. Thus, the transition between the Oie and Oa horizons may mark a transition between N-limited and C-limited microbial metabolisms. Considering the whole soil profile, faster turnover of N in the Oie horizon could plausibly result in greater leaching to lower soil horizons where inorganic N may accumulate in these presumably C-limited lower horizons, becoming susceptible to leaching during event flow. This would account for the fact that we observed higher inorganic N concentrations throughout the soil profile, despite no difference in gross or net N mineralization in these horizons. While we did not find a significant difference in SOM pool sizes between the reference and treatment watersheds, our sample sizes were likely far too small to reliably detect such a difference (Yanai et al. 2013), and the spatially and temporally intensive sampling of Johnson et al. (2014),

387 involving 20 times our sample numbers, should be considered a much more reliable indicator of
388 changes in SOM pool sizes.

389 To examine whether soil acid-base properties drove the increased N mineralization in the
390 Ca-enriched watershed, we looked for correlations between soil pH, Ca and Al with rates of N
391 cycling across both watersheds. There was a wide range in all of these variables both within and
392 between watersheds. For example, in the Oie horizon soils of the Ca-enriched watershed,
393 exchangeable Ca ranged from 93 to 267 $\mu mol_c\ gds^{-1}$, pH ranged from 4.15 to 4.68, and
394 exchangeable Al ranged from 0 to 2.45 $\mu mol_c\ gds^{-1}$. Lovett et al. (2016) proposed that Ca
395 limitation of white rot fungi may inhibit leaf litter decomposition, but we found no correlation
396 between exchangeable Ca and gross or net rates of N cycling in any soil horizon. Others have
397 proposed that low soil pH and associated Al toxicity may suppress soil microbial activity (Illmer
398 et al. 2003, Rousk et al. 2009), but we found no relationship between exchangeable Al or soil pH
399 and N cycling rates in any horizon. These results indicate that acid stress was not a strong control
400 on N cycling at the time of sampling. These results suggest that the direct geochemical effects of
401 the treatment are likely not the main cause of enhanced N cycling in the Ca-enriched watershed.

402 We did find evidence that the mechanism driving enhanced N turnover in the Ca-
403 enriched leaf litter has acted at a substantial lag, and this lag may suggest some possible
404 mechanisms of the enhanced N turnover. Whereas Groffman et al. (2006) found no treatment
405 effect on gross N mineralization rates one year after the treatment, here we report a 37% increase
406 in Oie horizon gross N mineralization, seventeen years after the treatment. A mechanism driving
407 this lag may be a gradual shift in forest composition. In the Ca-enriched watershed, sugar maple
408 biomass increased gradually but substantially in the ten years post-treatment, whereas beech
409 biomass decreased (Battles et al. 2014). Sugar maples have been previously shown to support

high litter turnover and losses of inorganic N (Lovett et al. 2002, Templer et al. 2005). The simultaneous increase in sugar maple and decreases in beech biomass represents a shift from an ectomycorrhizal-dominated community to an arbuscular mycorrhizal-dominated community, a shift that has been associated with higher C and N turnover and less retentive N cycling (Phillips et al. 2013, Averill and Hawkes 2016). Another possible mechanism to explain the increased leaf litter N cycling may be changes in the leaf litter chemistry of individual species, as leaf N content in sugar maple and yellow birch both increased after treatment (Lovett et al. 2016). These changes were more immediate, however, and so would not account for the observed lag. Alternatively, enhanced N cycling could be driven by the gradual recovery of soil fauna adapted to more alkaline conditions. The Ca treatment initially suppressed soil arthropod abundance (Fisk et al. 2006) but soil arthropods have not been measured since. While earthworms are known to be strongly sensitive to pH and to promote ecosystem C and N loss (Groffman et al. 2015), earthworm density in the Ca-enriched watershed is very low (Groffman, personal communication), making this mechanism unlikely. We conclude that the gradual change in forest composition is therefore the most plausible driver of enhanced N losses in the Ca-enriched watershed, although further work is needed to provide evidence for this hypothesis.

5. Conclusions

We have shown that experimental acid mitigation has the potential to unlock soil N stocks and enhance watershed N losses, and we suggest that this experimental mitigation may mimic deacidification that will occur naturally over timescales of decades to centuries. This calls for renewed attention to an old problem - acid rain may be a problem that has largely been solved in the developed world, but its legacy will likely continue to alter the C and N cycles of these forests for many decades to come. This is cause for significant concern, as the benefits of

deacidification may be accompanied by a decrease in the terrestrial C sink and an increase in N loading to receiving aquatic ecosystems. In order to anticipate these changes, there is a pressing need for models that predict changes to soil acidity and base cation fertility across different soil parent material geologies and acid deposition gradients, and to predict resultant changes in SOM dynamics.

Ecosystem deacidification is of course only a single process that may affect ecosystem N balance in systems that are experiencing multiple simultaneous anthropogenic forcings. Decreased nitrogen deposition may conversely drive more conservative ecosystem N cycling (Groffman et al. 2018), as would be predicted by classic hypotheses regarding ecosystem retention of limiting nutrients (Vitousek and Reiners 1975). Accelerated nitrogen cycling due to deacidification may thus be counterbalanced by more conservative N cycling due to reduced deposition. Others, however, have documented decreasing ecosystem N retention at many sites across United States despite declines in N deposition (Newcomer et al. 2021), and yet others have proposed that European forests may not respond strongly at all to decreasing N deposition (Schmitz et al. 2024). Like the lagged response to deacidification documented here, forest responses to decreased N deposition are likely to be lagged and exhibit hysteretic behavior (Gilliam et al. 2019). Further complicating ecosystem N balance are changes to hydroclimatic regimes that have altered patterns of N export (Bernal et al. 2012, Groffman et al. 2018, Lucas et al. 2106) as well as vegetation composition changes driven by exotic pests (Crowley and Lovett 2017). Disentangling the effects of ecosystem deacidification from these important other forcings, and understanding the timescales of lagged effects, will be central to determining the long-term trajectories of ecosystem N balance in acid-impacted forests.

Acknowledgements:

This work was funded in part by NSF award # 1637685. This work is a contribution of the Hubbard Brook Ecosystem Study. Hubbard Brook is part of the Long-Term Ecological Research (LTER) network, which is supported by the National Science Foundation. The Hubbard Brook Experimental Forest is operated and maintained by the U.S.D.A. Forest Service, Northern Research Station, Newtown Square, PA.

Data Statement:

All data used in this publication are available via the Environmental Data Initiative at: https://doi.org/10.6073/pasta/67c4e89f4c195029e3ff6062366143ba

References

Abreu Jr., C. H., T. Muraoka, and A. F. Lavorante. 2003. Exchangeable aluminum evaluation in acid soils. Scientia Agricola 60:543–548.

Averill, C., and C. V. Hawkes. 2016. Ectomycorrhizal fungi slow soil carbon cycling. Ecology Letters 19:937–947.

Bailey VL, Pries CH, Lajtha K. 2019. What do we know about soil carbon destabilization? Environ Res Lett 14:083004.

Battles, J. J., T. J. Fahey, C. T. Driscoll, J. D. Blum, and C. E. Johnson. 2014. Restoring Soil Calcium Reverses Forest Decline. Environmental Science & Technology Letters 1:15–19.

Bernal, S., L. O. Hedin, G. E. Likens, S. Gerber, and D. C. Buso. 2012. Complex response of the forest nitrogen cycle to climate change. Proceedings of the National Academy of Sciences:201121448.

Bernhardt, E. S., G. E. Likens, R. O. Hall, D. C. Buso, S. G. Fisher, T. M. Burton, J. L. Meyer, W. H. McDowell, M. S. Mayer, W. B. Bowden, S. E. G. Findlay, K. H. Macneale, R. S. Stelzer, and W. H. Lowe. 2005. Can't See the Forest for the Stream? In-stream Processing and Terrestrial Nitrogen Exports. BioScience 55:219–230.

Cho, Y., C. T. Driscoll, C. E. Johnson, and T. G. Siccama. 2010. Chemical changes in soil and soil solution after calcium silicate addition to a northern hardwood forest. Biogeochemistry 100:3–20.

Clarholm, M., and U. Skyllberg. 2013. Translocation of metals by trees and fungi regulates pH, soil organic matter turnover and nitrogen availability in acidic forest soils. Soil Biology and Biochemistry 63:142–153.

Coughlan, A. P., Y. Dalpé, L. Lapointe, and Y. Piché. 2000. Soil pH-induced changes in root colonization, diversity, and reproduction of symbiotic arbuscular mycorrhizal fungi from healthy and declining maple forests. Canadian Journal of Forest Research 30:1543–1554.

Crowley, K. F., and G. M. Lovett. 2017. Effects of nitrogen deposition on nitrate leaching from forests of the northeastern United States will change with tree species composition. Canadian Journal of Forest Research 47:997–1009.

Driscoll, C. T., K. M. Driscoll, H. Fakhraei, and K. Civerolo. 2016. Long-term temporal trends and spatial patterns in the acid-base chemistry of lakes in the Adirondack region of New York in response to decreases in acidic deposition. Atmospheric Environment 146:5–14.

Elrys AS, Ali A, Zhang H, Cheng Y, Zhang J, Cai Z-C, Müller C, Chang SX. 2021. Patterns and drivers of global gross nitrogen mineralization in soils. Global Change Biology 27:5950–62.

Erlandsson, M., N. Cory, J. Fölster, S. Köhler, H. Laudon, G. A. Weyhenmeyer, and K. Bishop. 2011. Increasing Dissolved Organic Carbon Redefines the Extent of Surface Water Acidification and Helps Resolve a Classic Controversy. BioScience 61:614–618.

Fahey, T. J. 2016. Coarse Litterfall Data at the Hubbard Brook Experimental Forest, 1996 - present. Environmental Data Initiative.

Fisk, M. C., W. R. Kessler, A. Goodale, T. J. Fahey, P. M. Groffman, and C. T. Driscoll. 2006. Landscape variation in microarthropod response to calcium addition in a northern hardwood forest ecosystem. Pedobiologia 50:69–78.

Geissen, V., and G. W. Brümmer. 1999. Decomposition rates and feeding activities of soil fauna in deciduous forest soils in relation to soil chemical parameters following liming and fertilization. Biology and Fertility of Soils 29:335–342.

Gilliam, F. S., D. A. Burns, C. T. Driscoll, S. D. Frey, G. M. Lovett, and S. A. Watmough. 2019. Decreased atmospheric nitrogen deposition in eastern North America: Predicted responses of forest ecosystems. Environmental Pollution 244:560–574.

Groffman, P. M. 2021. Microbial biomass and activity. https://portal.edirepository.org/nis/mapbrowse?scope=knb-lter-hbr&identifier=67.

Groffman, P. M., T. J. Fahey, M. C. Fisk, J. B. Yavitt, R. E. Sherman, P. J. Bohlen, and J. C. Maerz. 2015. Earthworms increase soil microbial biomass carrying capacity and nitrogen retention in northern hardwood forests. Soil Biology and Biochemistry 87:51–58.

Groffman, P. M., C. T. Driscoll, J. Durán, J. L. Campbell, L. M. Christenson, T. J. Fahey, M. C. Fisk, C. Fuss, G. E. Likens, G. Lovett, L. Rustad, and P. H. Templer. 2018. Nitrogen oligotrophication in northern hardwood forests. Biogeochemistry 141:523–539.

Groffman, P. M., M. C. Fisk, C. T. Driscoll, G. E. Likens, T. J. Fahey, C. Eagar, and L. H. Pardo. 2006. Calcium Additions and Microbial Nitrogen Cycle Processes in a Northern Hardwood Forest. Ecosystems 9:1289–1305.

Hall, S. J., and A. Thompson. 2022. What do relationships between extractable metals and soil organic carbon concentrations mean? Soil Science Society of America Journal 86:195–208.

Hart, S. C., G. E. Nason, D. D. Myrold, and D. A. Perry. 1994. Dynamics of Gross Nitrogen Transformations in an Old-Growth Forest: The Carbon Connection. Ecology 75:880–891.

Hobbie, S. E., M. Ogdahl, J. Chorover, O. A. Chadwick, J. Oleksyn, R. Zytkowiak, and P. B. Reich. 2007. Tree Species Effects on Soil Organic Matter Dynamics: The Role of Soil Cation Composition. Ecosystems 10:999–1018.

Hubbard Brook Watershed Ecosystem Record (HBWatER). 2021. Hubbard Brook Experimental Forest: Chemistry of Precipitation – Monthly Fluxes, Watershed 1, 1963 - present ver 11. Environmental Data Initiative. https://doi.org/10.6073/pasta/a446363d4a91dc8d5b10fd21b1d07b0c (Accessed 2023-11-29).

532 Illmer, P., U. Obertegger, and F. Schinner. 2003. Microbiological Properties in Acidic Forest Soils with
533 Special Consideration of KCl Extractable Al. Water, Air, and Soil Pollution 148:3–14.
534 Jenkinson, D. S., and D. S. Powlson. 1976. The effects of biocidal treatments on metabolism in soil—V:
535 A method for measuring soil biomass. Soil Biology and Biochemistry 8:209–213.
536 Johnson, C. E., C. T. Driscoll, J. D. Blum, T. J. Fahey, and J. J. Battles. 2014. Soil Chemical Dynamics
537 after Calcium Silicate Addition to a Northern Hardwood Forest. Soil Science Society of America
538 Journal 78:1458.
539 Johnson, C., and S. Hamburg. 2016. Mass and Chemistry of Organic Horizons and Surface Mineral
540 Soils on Watershed 6 at the Hubbard Brook Experimental Forest, 1976 - present. Environmental
541 Data Initiative.
542 Jones DL, Cooledge EC, Hoyle FC, Griffiths RI, Murphy DV. 2019. pH and exchangeable aluminum are
543 major regulators of microbial energy flow and carbon use efficiency in soil microbial
544 communities. Soil Biology and Biochemistry 138:107584.
545 Joslin, J. D., J. M. Kelly, and H. V. Miegroet. 1992. Soil Chemistry and Nutrition of North American
546 Spruce-Fir Stands: Evidence for Recent Change. Journal of Environmental Quality 21:12–30.
547 Judd, K. E., G. E. Likens, and P. M. Groffman. 2007. High Nitrate Retention during Winter in Soils of the
548 Hubbard Brook Experimental Forest. Ecosystems 10:217–225.
549 Juice, S. M., T. J. Fahey, T. G. Siccama, C. T. Driscoll, E. G. Denny, C. Eagar, N. L. Cleavitt, R.
550 Minocha, and A. D. Richardson. 2006. Response of sugar maple to calcium addition to northern
551 hardwood forest. Ecology 87:1267–1280.
552 Kätterer, T., M. Reichstein, O. Andrén, and A. Lomander. 1998. Temperature dependence of organic
553 matter decomposition: a critical review using literature data analyzed with different models.
554 Biology and Fertility of Soils 27:258–262.
555 Kirk, G. J. D., P. H. Bellamy, and R. M. Lark. 2010. Changes in soil pH across England and Wales in
556 response to decreased acid deposition. Global Change Biology 16:3111–3119.

Kooch, Y., S. M. Darabi, and S. M. Hosseini. 2015. Effects of Pits and Mounds Following Windthrow Events on Soil Features and Greenhouse Gas Fluxes in a Temperate Forest. Pedosphere 25:853–867.

Kothawala, D. N., and T. R. Moore. 2009. Adsorption of dissolved nitrogen by forest mineral soils. Canadian Journal of Forest Research 39:2381–2390.

Lawrence, G. B., P. W. Hazlett, I. J. Fernandez, R. Ouimet, S. W. Bailey, W. C. Shortle, K. T. Smith, and M. R. Antidormi. 2015. Declining Acidic Deposition Begins Reversal of Forest-Soil Acidification in the Northeastern U.S. and Eastern Canada. Environmental Science & Technology 49:13103–13111.

Lawrence, G. B., W. C. Shortle, M. B. David, K. T. Smith, R. A. F. Warby, and A. G. Lapenis. 2012. Early indications of soil recovery from acidic deposition in U.S. red spruce forests. Soil Science Society of America Journal 76:14071417.

Lawrence GB, Scanga SE, Sabo RD. 2020. Recovery of Soils From Acidic Deposition May Exacerbate Nitrogen Export From Forested Watersheds. Journal of Geophysical Research: Biogeosciences 125:e2019JG005036.

Lucas, R. W., R. A. Sponseller, M. J. Gundale, J. Stendahl, J. Fridman, P. Högberg, and H. Laudon. 2016. Long-term declines in stream and river inorganic nitrogen (N) export correspond to forest change. Ecological Applications 26:545–556.

Li Z, Zeng Z, Tian D, Wang J, Fu Z, Zhang F, Zhang R, Chen W, Luo Y, Niu S. 2020. Global patterns and controlling factors of soil nitrification rate. Global Change Biology 26:4147–57.

Li, Y., S. J. Chapman, G. W. Nicol, and H. Yao. 2018. Nitrification and nitrifiers in acidic soils. Soil Biology and Biochemistry 116:290–301.

Likens, G. E. 2013. Biogeochemistry of a Forested Ecosystem. 3rd edition. Springer Science & Business.

Likens, G. E., F. H. Bormann, and N. M. Johnson. 1969. Nitrification: importance to nutrient losses from a cutover forested ecosystem. Science (New York, N.Y.) 163:1205–1206.

582 Likens, G. E., C. T. Driscoll, and D. C. Buso. 1996. Long-Term Effects of Acid Rain: Response and
583 Recovery of a Forest Ecosystem. Science 272:244–246.
584 Liu, B., P. T. Mørkved, Å. Frostegård, and L. R. Bakken. 2010. Denitrification gene pools, transcription
585 and kinetics of NO, N2O and N2 production as affected by soil pH. FEMS Microbiology Ecology
586 72:407–417.
587 Lovett, G. M., M. A. Arthur, and K. F. Crowley. 2016. Effects of Calcium on the Rate and Extent of
588 Litter Decomposition in a Northern Hardwood Forest. Ecosystems 19:87–97.
589 Lovett, G. M., K. C. Weathers, and M. A. Arthur. 2002. Control of Nitrogen Loss from Forested
590 Watersheds by Soil Carbon:Nitrogen Ratio and Tree Species Composition. Ecosystems 5:712–
591 718.
592 Matschonat, G., and E. Matzner. 1996. Soil chemical properties affecting NH4+ sorption in forest soils.
593 Zeitschrift für Pflanzenernährung und Bodenkunde 159:505–511.
594 Monteith, D. T., J. L. Stoddard, C. D. Evans, H. A. de Wit, M. Forsius, T. Høgåsen, A. Wilander, B. L.
595 Skjelkvåle, D. S. Jeffries, J. Vuorenmaa, B. Keller, J. Kopácek, and J. Vesely. 2007. Dissolved
596 organic carbon trends resulting from changes in atmospheric deposition chemistry. Nature
597 450:537–540.
598 Mueller, K. E., D. M. Eissenstat, S. E. Hobbie, J. Oleksyn, A. M. Jagodzinski, P. B. Reich, O. A.
599 Chadwick, and J. Chorover. 2012. Tree species effects on coupled cycles of carbon, nitrogen, and
600 acidity in mineral soils at a common garden experiment. Biogeochemistry 111:601–614.
601 Newcomer, M. E., N. J. Bouskill, H. Wainwright, T. Maavara, B. Arora, E. R. Siirila-Woodburn, D.
602 Dwivedi, K. H. Williams, C. Steefel, and S. S. Hubbard. 2021. Hysteresis Patterns of Watershed
603 Nitrogen Retention and Loss Over the Past 50 years in United States Hydrological Basins. Global
604 Biogeochemical Cycles 35:e2020GB006777.
605 Niemi, R. M., and M. Vepsäläinen. 2005a. Stability of the fluorogenic enzyme substrates and pH optima
606 of enzyme activities in different Finnish soils. Journal of Microbiological Methods 60:195–205.

Niemi, R. M., and M. Vepsäläinen. 2005b. Stability of the fluorogenic enzyme substrates and pH optima of enzyme activities in different Finnish soils. Journal of Microbiological Methods 60:195–205.

Oleson, K., M. Lawrence, B. Bonan, B. Drewniak, M. Huang, D. Koven, S. Levis, F. Li, J. Riley, M. Subin, S. Swenson, E. Thornton, A. Bozbiyik, R. Fisher, L. Heald, E. Kluzek, J.-F. Lamarque, J. Lawrence, R. Leung, W. Lipscomb, P. Muszala, M. Ricciuto, J. Sacks, Y. Sun, J. Tang, and Z.-L. Yang. 2013. Technical description of version 4.5 of the Community Land Model (CLM).

Oulehle, F., C. D. Evans, J. Hofmeister, R. Krejci, K. Tahovska, T. Persson, P. Cudlin, and J. Hruska. 2011. Major changes in forest carbon and nitrogen cycling caused by declining sulphur deposition. Global Change Biology 17:3115–3129.

Pardo, L. H., C. Kendall, J. Pett-Ridge, and C. C. Y. Chang. 2004. Evaluating the source of streamwater nitrate using δ15N and δ18O in nitrate in two watersheds in New Hampshire, USA. Hydrological Processes 18:2699–2712.

Parton, J., M. Hartman, D. Ojima, and S. Schimel. 1998. DAYCENT and its land surface submodel: Description and testing. Global and Planetary Change:35–48.

Phillips, J. D., P. Šamonil, Ł. Pawlik, J. Trochta, and P. Daněk. 2017. Domination of hillslope denudation by tree uprooting in an old-growth forest. Geomorphology 276:27–36.

Phillips, R. P., E. Brzostek, and M. G. Midgley. 2013. The mycorrhizal-associated nutrient economy: a new framework for predicting carbon-nutrient couplings in temperate forests. The New Phytologist 199:41–51.

R Core Team. 2022. R: A Language and Environment for Statistical Computing. Vienna, Austria.

Reich, P. B., J. Oleksyn, J. Modrzynski, P. Mrozinski, S. E. Hobbie, D. M. Eissenstat, J. Chorover, O. A. Chadwick, C. M. Hale, and M. G. Tjoelker. 2005. Linking litter calcium, earthworms and soil properties: a common garden test with 14 tree species. Ecology Letters 8:811–818.

Rosi-Marshall, E. J., E. S. Bernhardt, D. C. Buso, C. T. Driscoll, and G. E. Likens. 2016. Acid rain mitigation experiment shifts a forested watershed from a net sink to a net source of nitrogen. Proceedings of the National Academy of Sciences 113:7580–7583.

633 Rousk, J., P. C. Brookes, and E. Bååth. 2009. Contrasting Soil pH Effects on Fungal and Bacterial
634 Growth Suggest Functional Redundancy in Carbon Mineralization. Applied and Environmental
635 Microbiology 75:1589–1596.
636 Rowley, M. C., S. Grand, and É. P. Verrecchia. 2018. Calcium-mediated stabilisation of soil organic
637 carbon. Biogeochemistry 137:27–49.
638 Rowley, M. C., P. S. Nico, S. E. Bone, M. A. Marcus, E. F. Pegoraro, C. Castanha, K. Kang, A.
639 Bhattacharyya, M. S. Torn, and J. Peña. 2023. Association between soil organic carbon and
640 calcium in acidic grassland soils from Point Reyes National Seashore, CA. Biogeochemistry
641 165:91–111.
642 Schaetzl, R. J., S. F. Burns, D. L. Johnson, and T. W. Small. 1988. Tree uprooting: review of impacts on
643 forest ecology. Vegetatio 79:165–176.
644 Schmidt, M. W. I., M. S. Torn, S. Abiven, T. Dittmar, G. Guggenberger, I. A. Janssens, M. Kleber, I.
645 Kögel-Knabner, J. Lehmann, D. A. C. Manning, P. Nannipieri, D. P. Rasse, S. Weiner, and S. E.
646 Trumbore. 2011. Persistence of soil organic matter as an ecosystem property. Nature 478:49–56.
647 Schmitz, A., T. G. M. Sanders, A. Bolte, F. Bussotti, T. Dirnböck, J. Peñuelas, M. Pollastrini, A.-K.
648 Prescher, J. Sardans, A. Verstraeten, and W. de Vries. 2024. Chapter 13 - Responses of forest
649 ecosystems in Europe to decreasing nitrogen deposition. Pages 227–245 in E. Du and W. de
650 Vries, editors. Atmospheric Nitrogen Deposition to Global Forests. Academic Press.
651 Shabtai, I. A., R. C. Wilhelm, S. A. Schweizer, C. Höschen, D. H. Buckley, and J. Lehmann. 2023.
652 Calcium promotes persistent soil organic matter by altering microbial transformation of plant
653 litter. Nature Communications 14:6609.
654 Simek, M., and J. E. Cooper. 2002. The influence of soil pH on denitrification: progress towards
655 the understanding of this interaction over the last 50 years. European Journal of Soil Science
656 53:345–354.
657 Slessarev, E. W., Y. Lin, N. L. Bingham, J. E. Johnson, Y. Dai, J. P. Schimel, and O. A. Chadwick. 2016.
658 Water balance creates a threshold in soil pH at the global scale. Nature 540:567–569.

659 Sørensen, P., and E. S. Jensen. 1991. Sequential diffusion of ammonium and nitrate from soil extracts to a
660 polytetrafluoroethylene trap for 15N determination. Analytica Chimica Acta 252:201–203.
661 Stempfhuber, B., M. Engel, D. Fischer, G. Neskovic-Prit, T. Wubet, I. Schöning, C. Gubry-Rangin, S.
662 Kublik, B. Schloter-Hai, T. Rattei, G. Welzl, G. W. Nicol, M. Schrumpf, F. Buscot, J. I. Prosser,
663 and M. Schloter. 2015. pH as a Driver for Ammonia-Oxidizing Archaea in Forest Soils.
664 Microbial Ecology 69:879–883.
665 Sullivan, T. J., G. B. Lawrence, S. W. Bailey, T. C. McDonnell, C. M. Beier, K. C. Weathers, G. T.
666 McPherson, and D. A. Bishop. 2013. Effects of acidic deposition and soil acidification on sugar
667 maple trees in the Adirondack Mountains, New York. Environmental Science & Technology
668 47:12687–12694.
669 Templer, P. H., G. M. Lovett, K. C. Weathers, S. E. Findlay, and T. E. Dawson. 2005. Influence of Tree
670 Species on Forest Nitrogen Retention in the Catskill Mountains, New York, USA. Ecosystems
671 8:1–16.
672 Thornton, P. E., S. W. Running, and E. R. Hunt. 2005. Biome-BGC: Terrestrial Ecosystem Process
673 Model, Version 4.1.1. ORNL DAAC.
674 Tierney, G. L., and T. J. Fahey. 2002. Fine root turnover in a northern hardwood forest: a direct
675 comparison of the radiocarbon and minirhizotron methods. Canadian Journal of Forest Research
676 32:1692–1697.
677 Valtera, M., and R. J. Schaetzl. 2017. Pit-mound microrelief in forest soils: Review of implications for
678 water retention and hydrologic modelling. Forest Ecology and Management 393:40–51.
679 Veneman, P. L. M., P. V. Jacke, and S. M. Bodine. 1984. Soil formation as affected by pit and mound
680 microrelief in Massachusetts, USA. Geoderma 33:89–99.
681 Venterea, R. T., P. M. Groffman, L. V. Verchot, A. H. Magill, and J. D. Aber. 2004. Gross nitrogen
682 process rates in temperate forest soils exhibiting symptoms of nitrogen saturation. Forest Ecology
683 and Management 196:129–142.

Vitousek, P. M., and W. A. Reiners. 1975. Ecosystem Succession and Nutrient Retention: A Hypothesis. BioScience 25:376–381.

Yanai, R. D., M. A. Vadeboncoeur, S. P. Hamburg, M. A. Arthur, C. B. Fuss, P. M. Groffman, T. G. Siccama, and C. T. Driscoll. 2013. From Missing Source to Missing Sink: Long-Term Changes in the Nitrogen Budget of a Northern Hardwood Forest. Environmental Science & Technology 47:11440–11448.

691 **Tables**

692 **Table 1: Soil properties related to soil C cycling.** Means and standard errors (in parentheses) are reported.

	Watershed	GWC (%)	SOM (%)	C Mineralization (μg C gds^{-1} d^{-1})	Microbial Biomass (mg gds^{-1})
Summer 2015					
Oie horizon	Reference	67.0 (2.0)	71.3 (3.9)	617 (85)	13.2 (1.0)
	Ca-enriched	69.4 (1.5)	73.8 (1.7)	657 (40)	14.5 (1.4)
Oa horizon	Reference	54.3 (2.1)	34.2 (3.0)	89.4 (6.6)	3.54 (0.27)
	Ca-enriched	51.2 (2.4)	31.6 (3.5)	93.3 (11.0)	3.59 (0.41)
0-10 cm mineral soil	Reference	34.8 (1.6)	10.9 (0.6)	17.4 (0.98)	0.803 (0.076)
	Ca-enriched	34.9 (0.81)	11.7 (0.5)	16.6 (1.20)	0.801 (0.071)
Spring 2016					
Oie horizon	Reference	66.9 (2.3)	73.8 (4.4)	742.0 (82)	13.4 (0.93)
	Ca-enriched	70.8 (1.8)	77.2 (2.1)	880 (58)	15.8 (1.5)
Oa horizon	Reference	57.5 (2.3)	39.7 (4.2)	99.7 (13)	4.04 (0.26)
	Ca-enriched	59.6 (3.0)	44.0 (5.4)	112.0 (20)	4.51 (0.57)
0-10 cm mineral soil	Reference	34.8 (2.1)	10.6 (0.9)	16.3 (1.7)	0.794 (0.088)
	Ca-enriched	35.2 (1.7)	10.6 (0.5)	14.5 (1.1)	0.839 (0.110)

693
694

Figures

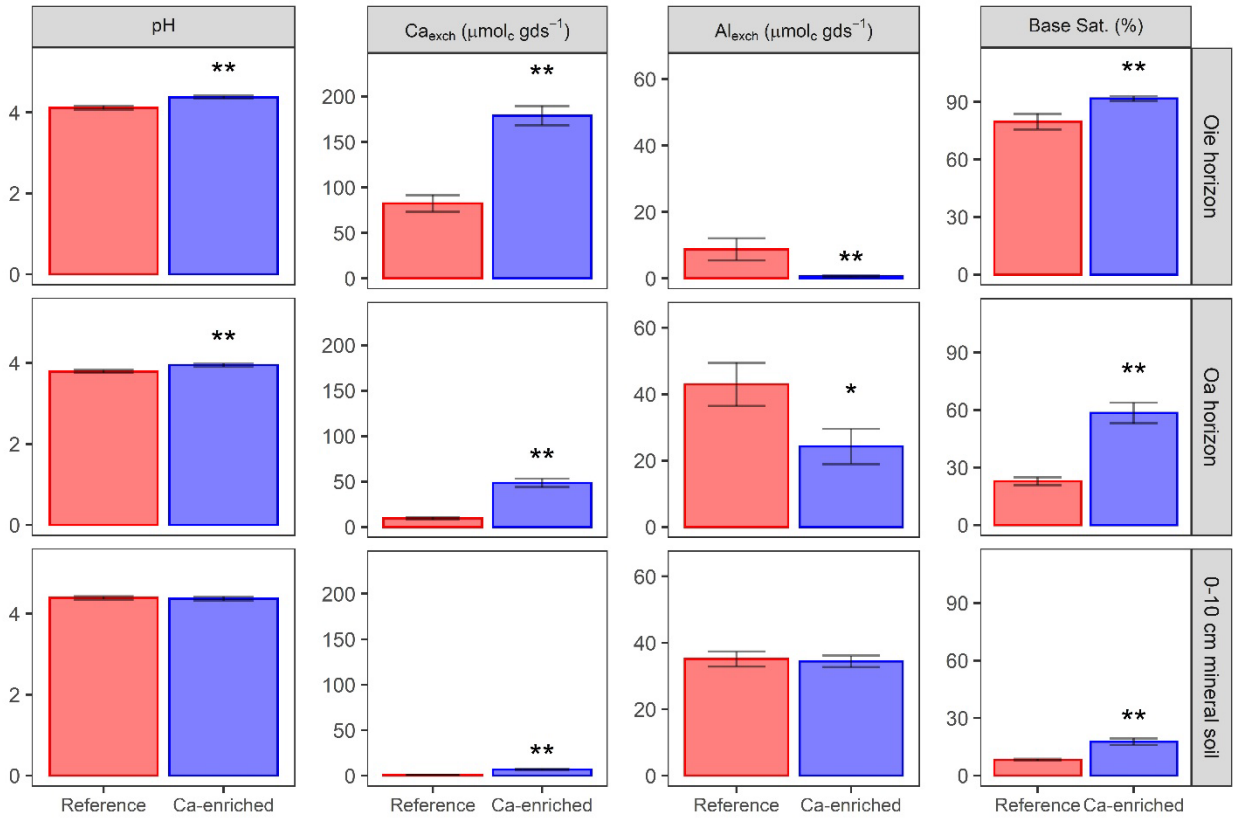

Figure 1: Soil acid-base properties. Means and standard errors are displayed. Asterisks indicate a significant difference between the Ca-enriched watershed and the reference watershed (* $p < 0.10$, ** $p < 0.05$). Soil pH and exchangeable Ca data are aggregated from spring and summer sampling dates. Exchangeable Al and base saturation are data from the spring sampling date only.

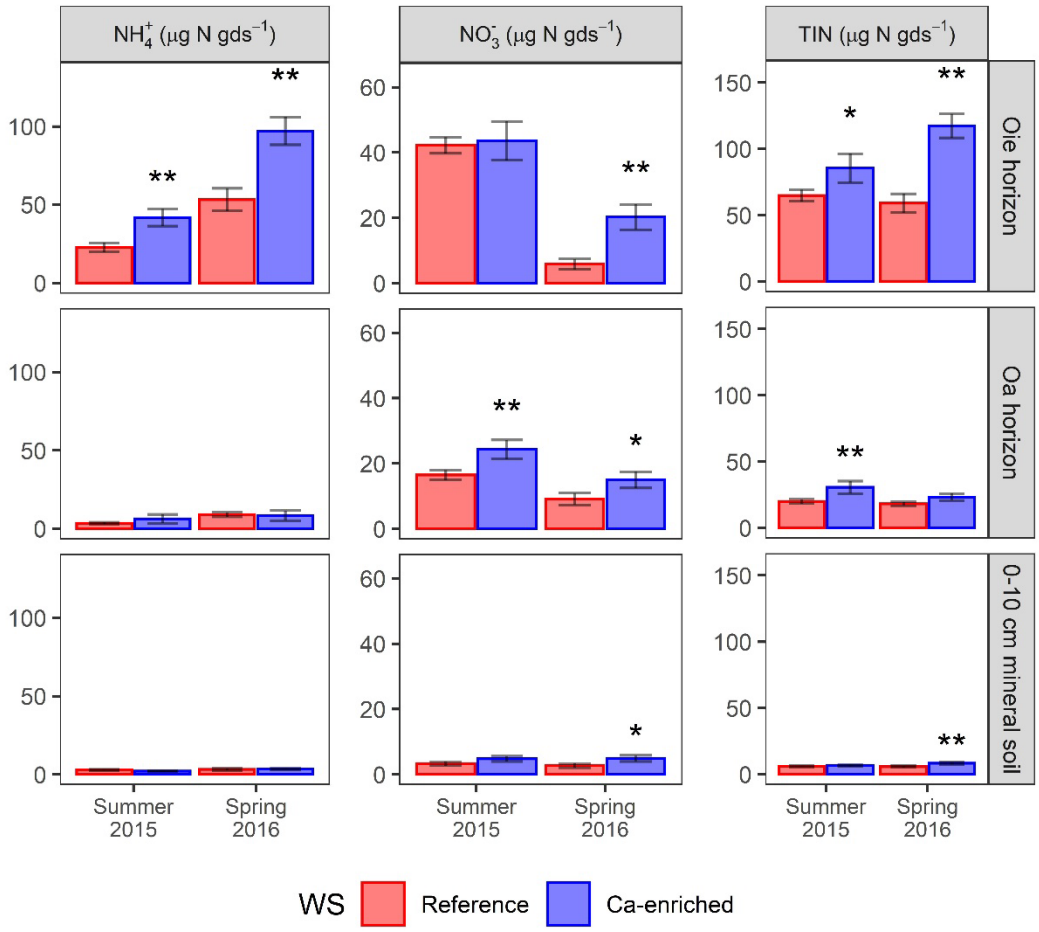

701

702 **Figure 2:** Soil inorganic N concentrations by horizon. Means and standard errors are displayed.

703 Asterisks indicate a significant difference between the Ca enriched watershed and the reference

704 watershed (* $p < 0.10$, ** $p < 0.05$).

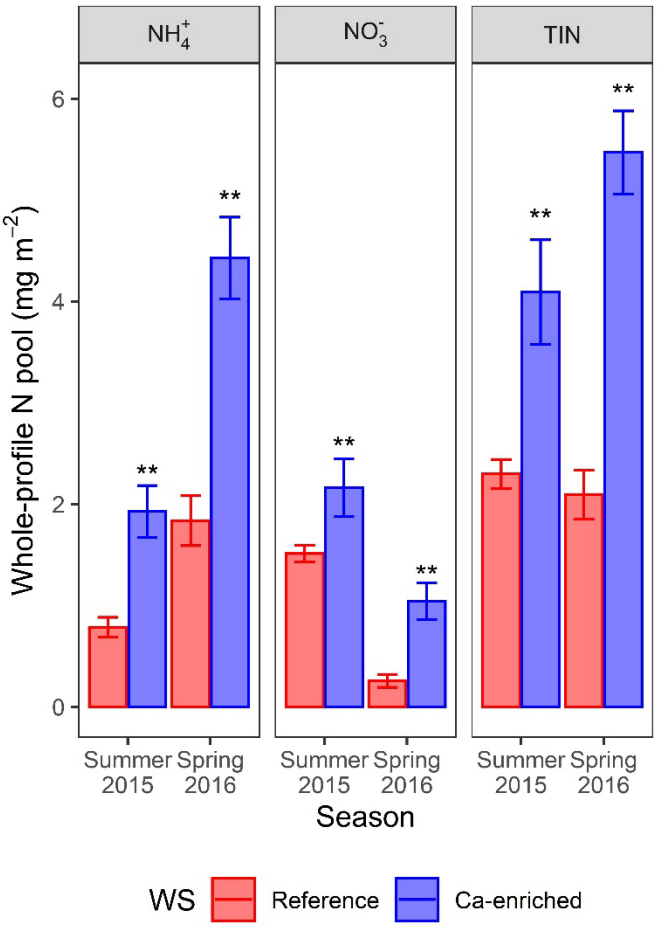

705

706 **Figure 3:** Whole-profile soil inorganic N pools for the forest floor and 0 - 10 cm mineral soil.

707 Means and standard errors are displayed. Asterisks indicate a significant difference between the

708 Ca enriched watershed and the reference watershed ($p < 0.05$).

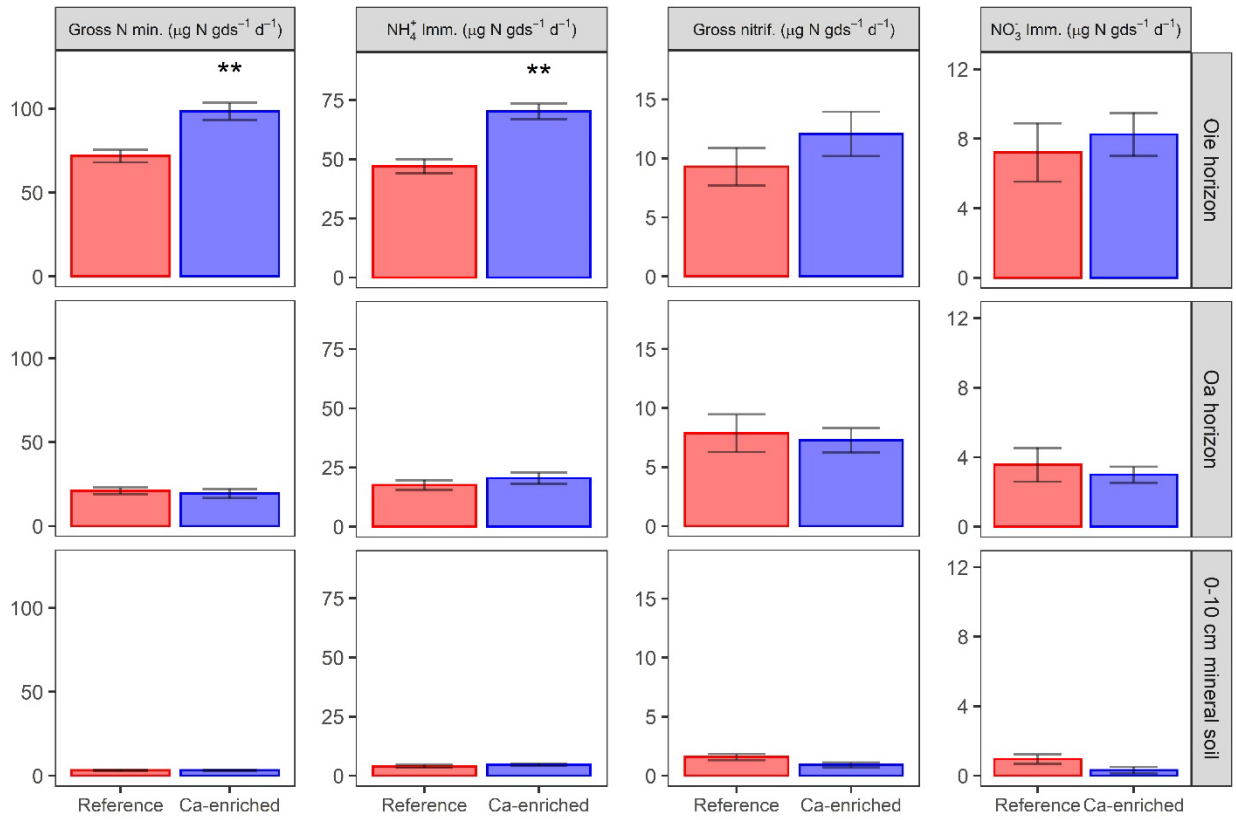

709

710 **Figure 4:** Gross N cycling rates by horizon for spring 2016 soil samples. Asterisks indicate a

711 significant difference between the Ca enriched watershed and the reference watershed ($p < 0.05$).

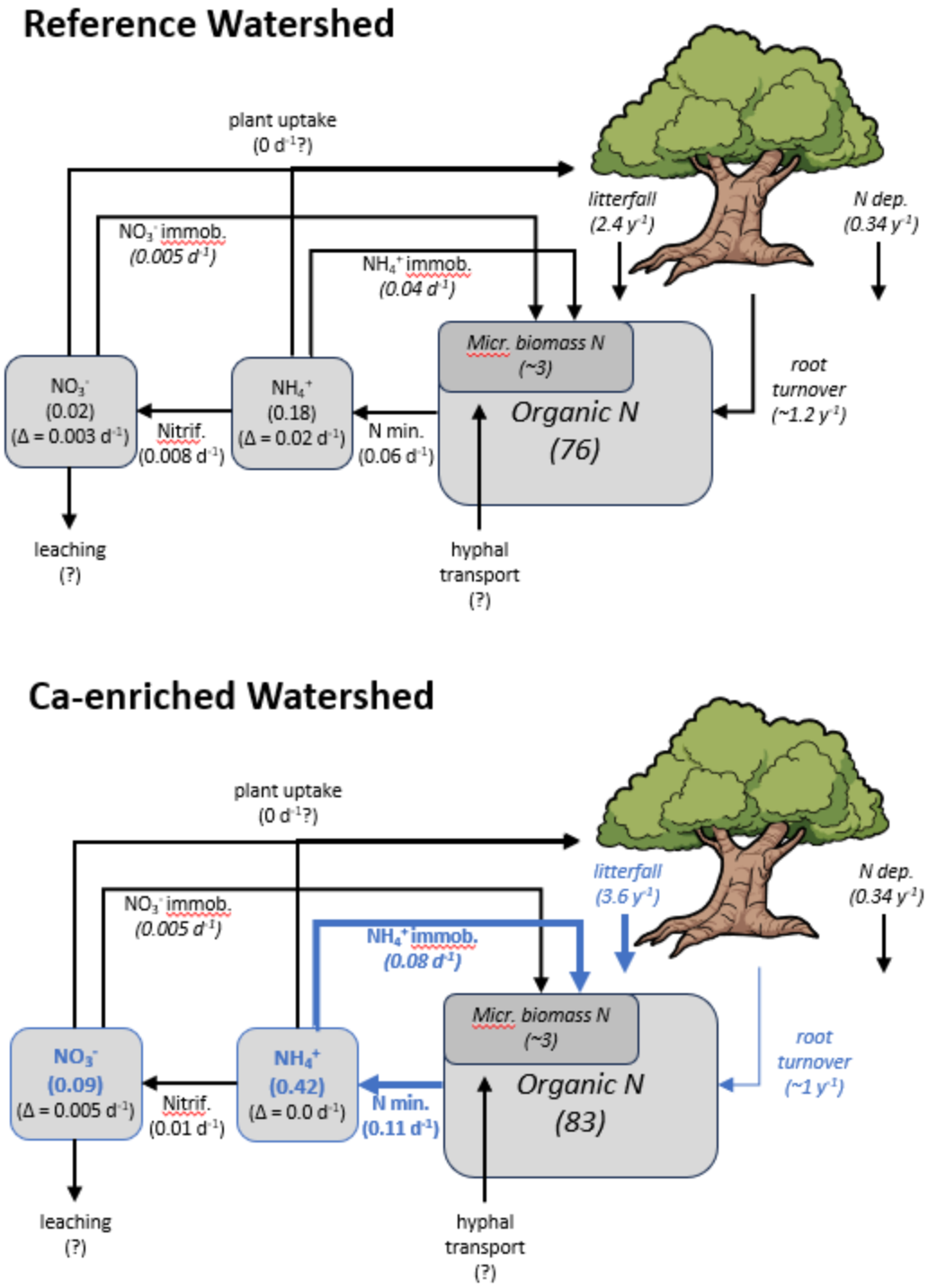

712

713 **Figure 5:** A N budget "snapshot" for the Oie horizon in spring 2016, reflecting the differences in

714 N pools and gross process rates that we measured. All pools are in units of g m^{-2} and fluxes are in

715 units of g m^{-2} per unit time indicated. Italics indicate pools or fluxes taken or computed from the
716 literature. Blue text indicates a pool or flux that is significantly different between the Ca-enriched
717 and reference watersheds (as either analyzed here or in the cited literature.)

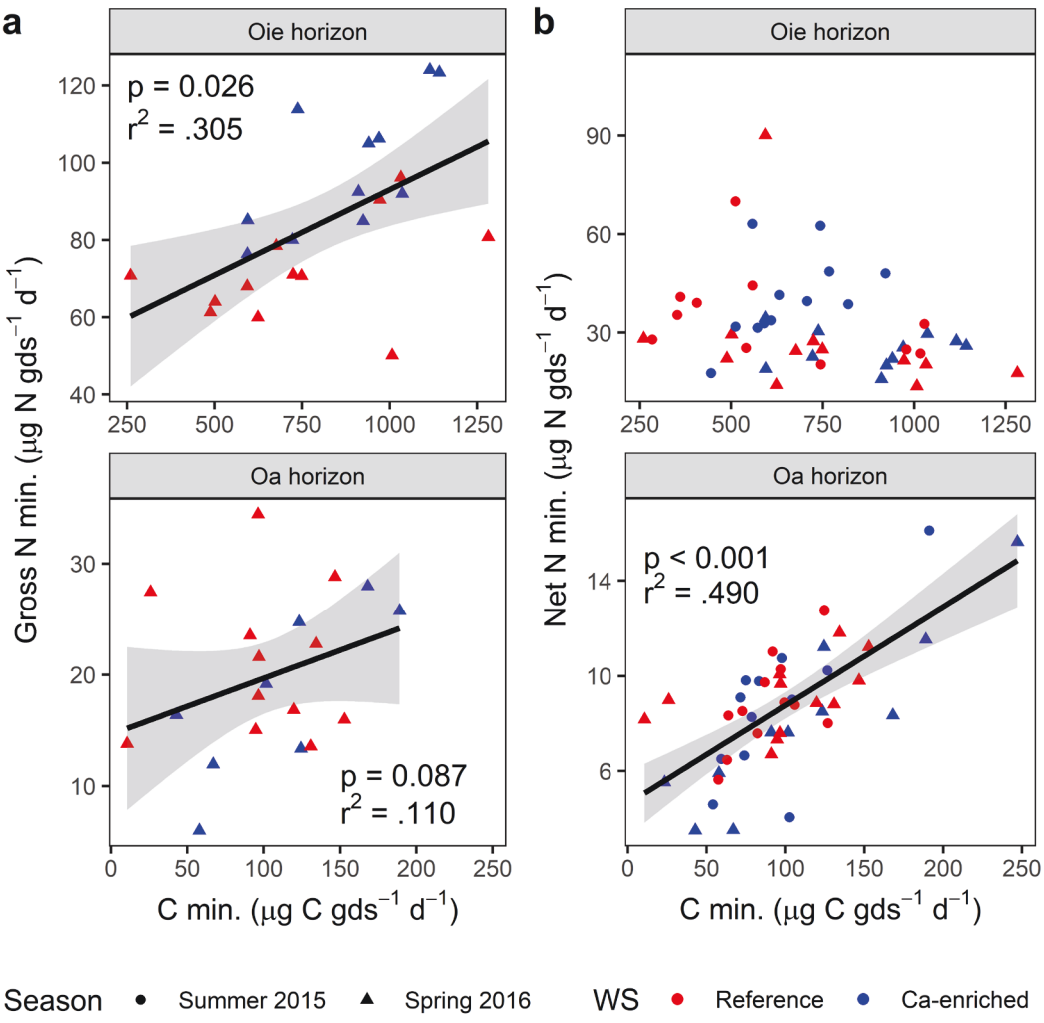

718

719 **Figure 6:** Correlations between C mineralization and (a) gross and (b) net N mineralization for
720 forest floor soil samples. The significance of the correlation is reported for a full model that
721 included blocking factors for watershed, topographic position, and season, but the correlation
722 coefficient and linear regression displayed here are for the main predictor (C mineralization) only.
723 Only significant linear relationships are shown.

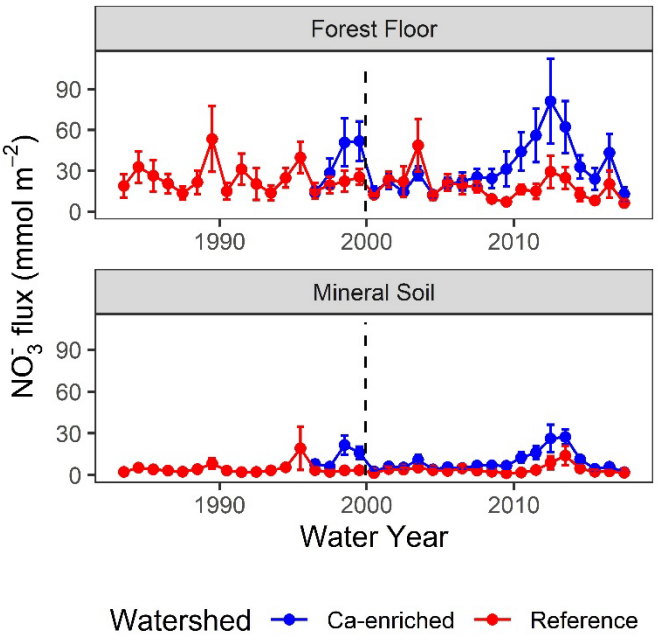

724

725 **Figure 7:** Soil solution total nitrogen (TN) fluxes for the forest floor (bottom of Oa horizon) and

726 mineral soil. Error bars are ± 1 S.E.M.